Biochemical Pharmacology 83 (2012) 218–227

Contents lists available at SciVerse ScienceDirect

Biochemical Pharmacology

journal homepage: www.elsevier.com/locate/biochempharm

Inhibition of genotoxic stress induced apoptosis by novel TAT-fused peptides targeting PIDDosome

Tae-Ho Jang [b,1], Sung-Jun Lee [c,1], Chang-Hoon Woo [d], Kyung Jin Lee [e], Ju-Hong Jeon [f], Dong-Sup Lee [h], Kihang Choi [j], In-Gyu Kim [g], Young Whan Kim [i], Tae-Jin Lee [c], Hyun Ho Park [a,b,*]

[a] School of Biotechnology at Yeungnam University, Gyeongsan, South Korea
[b] Graduate School of Biochemistry at Yeungnam University, Gyeongsan, South Korea
[c] Department of Anatomy, College of Medicine, Yeungnam University, Daegu, South Korea
[d] Pharmacology, College of Medicine, Yeungnam University, Daegu, South Korea
[e] Department of Biological Science, College of Arts and Science, Cornell University, USA
[f] Department of Physiology, Seoul National University College of Medicine, and Institute of Dermatological Science, Medical Research Center, Seoul National University, Seoul, South Korea
[g] Department of Biochemistry and Molecular Biology/Aging and Apoptosis Research Center (AARC), Seoul National University College of Medicine, Seoul, South Korea
[h] Cancer Research Institute, Seoul National University College of Medicine, Seoul, South Korea
[i] Division of Pulmonary and Critical Care Medicine, Department of Internal Medicine and Lung Institute of Medical Research Center, Seoul National University College of Medicine, Seoul, South Korea
[j] Department of Chemistry, Korea University, Seoul, South Korea

ARTICLE INFO

Article history:
Received 26 August 2011
Accepted 17 October 2011
Available online 25 October 2011

Keywords:
Apoptosis
Caspase-2
RAIDD
PIDD
PIDDosome
Cisplatin
TAT-fused peptides

ABSTRACT

Genotoxic stress induced apoptosis is mediated by the formation of PIDDosome, which is a caspase-2 activating complex composed of three protein components, PIDD, RAIDD, and caspase-2. Here, synthetic TAT-fused peptides designed by the structure of PIDD and RAIDD, TAT-Y814A and TAT-R147E, respectively, were produced and tested for their ability to inhibit PIDDosome formation in vitro as well as to attenuate genotoxic stress-induced apoptosis in human renal cancer cells. The results show that TAT-Y814A and TAT-R147E have the potential to inhibit formation of the PIDDosome in a dose-dependent manner. Furthermore, both peptides partially inhibit genotoxic stress mediated apoptosis and activation of caspase2 and caspase3 in Caki cells. These results suggest that TAT-Y814A (also TAT-R147E) is a novel inhibitor of genotoxic stress-induced apoptosis that may serve as a prototype for anti-apoptotic drug development.

1. Introduction

Apoptosis, which is the process of programmed cell death, is involved in various physiological processes such as tissue homeostasis and embryonic development, as well as many human diseases [1,2]. Excessive apoptosis causes atrophy and neuronal degenerative diseases, whereas insufficient apoptosis results in many types of cancer [3–5].

This important process is mediated by the sequential activation of caspases, which can be classified into two groups according to their sequence of activation, initiator caspases (such as caspases-2, 8, 9 and 10) and effector caspases (such as caspases-3 and 7) [6–9]. Initiator caspases containing N-terminal pro-domains for the formation of caspase activating complexes are activated by a proximity induced self activation mechanism, whereas effector caspases are activated by activated initiator caspases [10–12]. Well-known initiator caspase activating complexes include DISC (Death Inducing Signaling Complex) for the activation of caspases-8 and 10 [13,14], apoptosome for the activation of caspase-9 [15,16], inflammasome for the activation of caspase-1 [17,18], and PIDDosome for the activation of caspase-2 [19,20]. Oligomerization of initiator caspases into complexes provides the proximity required for their self-activation.

PIDDosome is known to be composed of three proteins, PIDD, RAIDD, and caspase-2 [19,21]. PIDDosome is assembled in response to genotoxic-stress and leads to caspase-2-dependent apoptosis [19]. Interestingly, the activation of caspase-2 is not strictly dependent on the formation of PIDDosome. It has been shown that the activation of caspase-2 can occur due to dimerization, post-translational modification or an increase of

* Corresponding author at: School of Biotechnology and Graduate School of Biochemistry at Yeungnam University, Gyeongsan, South Korea.
Tel.: +82 53 810 3045; fax: +82 53 810 4769.
E-mail address: hyunho@ynu.ac.kr (H.H. Park).
[1] These authors contributed equally to this work.

0006-2952/$ – see front matter. Crown Copyright © 2011 Published by Elsevier Inc. All rights reserved.
doi:10.1016/j.bcp.2011.10.013

protein concentration [22–24]. This PIDDosome independent caspase-2 activation may indicate that alternative modes of caspase-2 activation may exist in the cell [24].

PIDD contains 910 residues with seven leucine rich repeats (LRRs), two ZU-5 domains and a c-terminal death domain (DD) [25]. Caspase-2 is the most evolutionarily conserved caspase across species of animals [26]; however, due to the lack of a distinct phenotype in knock-out mice there has been little interest in this caspase. Nevertheless, identification of the PIDDosome as a caspase-2 activating complex has shown that caspase-2 acts upstream of the mitochondrial pathway in response to genotoxic stress to induce caspase-2 mediated apoptosis [27,28], which has renewed interest in this field. Caspase-2 possesses the Caspase Recruiting Domain (CARD) at its N-terminus. PIDD is essential for cell death, which it facilitates by activating caspase-2. PIDD is also critical for cell survival via interaction with RIP1, a kinase that has been implicated in the activation of NF-κB [29,30]. The results of several studies have suggested that PIDD may be a molecular switch that controls the balance between life and death upon genotoxic stress [30]. RAIDD is an adapter protein that contains CARD domain at the N-terminus and a DD domain at the C-terminus [31]. The assembly of PIDDosome is completely dependent on the protein–protein interacting module known as the death-domain superfamily, which is composed of four subfamilies, the Death Domain (DD), Death Effector Domain (DED), Caspase-Recruitment Domain (CARD), and Pyrin Domain (PYD) [32]. PIDD and RAIDD interact via a DD:DD interaction, and RAIDD then recruits caspase-2 via a CARD:CARD interaction. The molecular structure of the core portion of the PIDDosome formed by seven RAIDD DD and five PIDD DD was recently elucidated [20]. Although the structure of the PIDDosome provided a great deal of information enabling a better understanding of its oligomerization mechanism at the core, there is still little biochemical information available regarding its assembly mechanism.

Recently, Jang and Park studied two important mutations, R147E and Y814A, on RAIDD DD and PIDD DD [33]. These mutations not only impair PIDDosome formation, but also exert a dominant negative effect on formation of the complex [33]. Here, we designed a TAT-fused peptide based on previously studied dominant negative mutants known as TAT-R147E and TAT-Y814A and showed their effects on the formation of PIDDosome, caspase-2 activation, and apoptosis induction. Our experiments clearly demonstrated that TAT-Y814A and TAT-R147E potently inhibited formation of the PIDDosome in a dose-dependent manner. Furthermore, both peptides slightly inhibited genotoxic stress-induced apoptosis in Caki cells. The effect of TAT-Y814A was relatively stronger than that of TAT-R147E. These results suggest that TAT-Y814A and TAT-R147E are novel genotoxic stress-induced apoptosis inhibitors that may serve as a prototype for anti-apoptotic drug development.

2. Materials and methods

2.1. Materials

pET vector was from Novagen (Madison, WI). All the restriction enzyme used for this study were from New England BioLabs (NEB) (Beverly, MA). *IPTG* and Triton-X100 were from Sigma–Aldrich (St. Louis, MO). Dulbecco's modified Eagle's medium (DMEM), fetal bovine serum (FBS) and antibiotics (Penicillin and Streptomycin) were purchased from Gibco BRL (Rockville, MD). Anti-caspase2 antibody and anti-caspase3 antibody were obtained from Santa Cruz (CA). Propidium iodide (PI) was obtained from Sigma Chemical Co.

2.2. Protein expression and purification

The cDNA of full length human RAIDD (1–199: RAIDD-FL) was used as a template for PCR and plasmid vector pET26b (Novagen) was used to add a hexa-histidine tag to the carboxy-terminus of RAIDD for affinity purification. PCR products of RAIDD-FL were digested with NdeI and XhoI (NEB) restriction enzymes and ligated into pET26b. The cloning process for RAIDD DD (94–199) and PIDD DD (777–883) was introduced elsewhere [20].

Recombinant RAIDD DD and PIDD DD was expressed in *Escherichia coli* BL21 (DE3) RILP and purified as previously described [20]. RAIDD-FL was expressed in the BL21 (DE3) *E. coli* line. The purification process for RAIDD-FL was similar to the process used for RAIDD DD. Briefly, the expression was induced by 0.5 mM isopropyl-β-D-thiogalactopyranoside (IPTG) overnight at 20 °C. The bacteria were then collected, resuspended and lysed by sonication in 50 ml lysis buffer (20 mM Tris–HCl at pH 7.9, 500 mM NaCl, 20 mM imidazole, and 5 mM β-ME). The cell debris was removed by centrifugation at 16,000 rpm for 60 min at 4 °C. The His-tagged target was purified by affinity chromatography using Ni-NTA beads (Qiagen) and gel-filtration chromatography using S-200 (GE Healthcare) pre-equilibrated with buffer containing 20 mM Tris–HCl pH 8.0, 150 mM NaCl, and 1 mM DTT.

2.3. Solubility assay

The general strategy of the solubility assay was based on the method described by Bondos and Bicknell (2003) [34]. Briefly, RAIDD-FL from gel-filtration chromatography in 20 mM Tris–HCl, 150 mM NaCl, 1 mM DTT buffer was incubated at various pH values (from pH 5 to 11) for 1 day at 4 °C. Approximately 300 μl of each 400 μl sample was used for a turbidity assay, in which the turbidity of each sample was measured directly based on the optical density at 600 nm using a spectrophotometer (Backman). The remaining 100 μl were used for an aggregation assay. The % aggregation was determined by both SDS-PAGE and a Bradford assay (Bio-Rad, Richmond, CA). For this experiment, each sample, which contained RAIDD-FL precipitates, was centrifugated at 10,000 × *g* and 4 °C for 20 min. Precaution was taken to avoid foam formation throughout all processes. RAIDD-FL remaining in the supernatant following centrifugation was defined as the soluble RAIDD. The decrease in RAIDD-FL by the removal of aggregates by centrifugation was detected by SDS-PAGE. All samples were boiled for 10 min at 90 °C prior to SDS-PAGE. Coomassie Brilliant Blue was used for staining and detection of bands on the acrylamide gels. Decreased RAIDD-FL was also quantitatively measured by calculating the protein concentration.

2.4. Complex association and dissociation assay by gel-filtration chromatography

Purified RAIDD-FL was pre-incubated with PIDD DD for 30 min at room temperature and the mixture was then subjected to a gel-filtration column equilibrated with buffers with various pH values. The % of the complex was evaluated based on the appearance and height of the complex peak at 280 nm. The amount of the complex formed at pH 8 was considered to be 100% complex.

A complex dissociation assay using TAT-Y814A peptides was conducted as follows. Separately purified and quantified RAIDD-FL, PIDD DD and TAT-Y814A were incubated for 60 min at room temperature. Following pre-incubation, the mixture was concentrated to 15–20 mg ml^{-1} using a concentration kit (Millipore). The concentrated protein mixture was then applied to a Superdex 200 gel-filtration column 10/30 (GE Healthcare), which was pre-equilibrated with a solution of 20 mM Tris buffer at pH 8.0 and 50 mM NaCl. Formation of the complex was then detected by

evaluating the positions of the eluted peak followed by SDS-PAGE. 100 μl of 1/10 diluted stock peptides (30 mg ml^{-1}) were used for this assay.

2.5. Peptide synthesis

Cell-permeable peptides containing RAIDD helix3 (GLSQTDIY**R** CKANHPHNV) and PIDD helix3 (GVS**Y**REVQRIRHEFR) fused to the internalization sequence of TAT transactivator domain (YGRKKRRQRRR) at their N-termini were synthesized and purified by ANYGEN (Gwangju, South Korea). Linker (GGG) was introduced between the TAT sequence and helix. N-terminally FITC (fluorescein isothiocyanate) attached peptides were synthesized and purified by Peptron (Dae-jeon, South Korea). The part of DREP2 (EYFRTLANNTVLLLLR), which is the regulator of apoptotic DNA fragmentation, was also fused to TAT sequence via linker. DREP2 derived TAT-fused peptide (YGRKKRRQRRRGGGEYFRTLANNTVLLLLR) was used for control experiment.

2.6. Complex dissociation assay by Native-PAGE

Formation of the complex between RAIDD DD/RAIDD-FL and PIDD DD was assayed by native (non-denaturing) PAGE conducted on a PhastSystem (GE Healthcare) with pre-made 8-25% acrylamide gradient gels (GE Healthcare). Coomassie Brilliant Blue was used for staining and detection of the shifted bands.

RAIDD DD:PIDD DD and RAIDD-FL:PIDD DD complexes were prepared in Tris buffer (20 mM Tris pH 8.0 and 50 mM NaCl). This complex was then pre-incubated with TAT-fused peptides for 60 min, after which the mixture was subjected to the gel. The % of the complex was evaluated based on the appearance of newly formed bands. The amount of the complex formed without TAT-R147E and TAT-Y814A was considered to be 100%.

2.7. Cell culture and immunoblotting

The human renal cancer Caki cells were cultured in DMEM medium supplemented with 10% fetal calf serum and Penicillin 100 Units/ml and Streptomycin 100 μg/ml. For the experiments, cells were seeded at into 6-well plates (Corning, Corning, NY) at 2×10^6 cells per well. Investigation of the cisplatin-induced apoptosis was conducted by pre-incubating cells with TAT fusion proteins (50 μM) such as TAT-Y814A, TAT-R147E, and TAT-DREP2 for 30 min prior to the addition of apoptotic stimulus. After incubated with 32 g/ml cisplatin for 12 h, cellular lysates were prepared by suspending 2×10^6 cells in 100 μl of lysis buffer (137 mM NaCl, 15 mM EGTA, 0.1 mM sodium orthovanadate, 15 mM $MgCl_2$, 0.1% Triton-X100, 25 mM MOPS, 100 μM phenylmethylsulfonyl fluoride, and 20 μM leupeptin, adjusted to pH 7.9). The cells were disrupted by sonication and extracted at 4 °C for 30 min. The proteins were then electro-transferred to Immobilon-P membranes (Millipore Corporation, Bedford, MA, USA). Detection of specific proteins was conducted using an ECL Western blotting kit according to the manufacturer's instructions.

2.8. Flow cytometry analysis

Apoptosis was quantified by fluorescence-activated cell sorting (FACS) analysis. Approximately 1×10^6 Caki cells were suspended in 100 μl of PBS, after which 200 μl of 95% ethanol were added and the samples were vortexed. The cells were then incubated at 4 °C for 60 min, washed with PBS, and resuspended in 250 μl of 1.12% sodium citrate buffer (pH 8.4) with 12.5 μg of RNase. Incubation was continued at 37 °C for 30 min. The cellular DNA was then stained by applying 250 μl of propidium iodide (50 μg/ml) for 30 min at room temperature. Finally, the stained cells were analyzed by FACS on a FACScan flow cytometer for relative DNA content based on red fluorescence.

2.9. Immunofluorescence staining

Caki cells were grown on glass coverslips and transduced with FITC-labeled peptides. After 24 h later, the cells were washed with PBS, fixed in 4% paraformaldehyde and permeabilized with 0.2% Triton-X100. Washed again with PBS, the coverslips were pre-incubated with 300 nM 4,6-diamidino-2-phenylindole (DAPI, Roche, Germany) in PBS for 5 min at room temperature. After washing with PBS, cells were examined by an inverted Leica CTR 6000 fluorescence microscope (Leica UK, Milton Keynes) using appropriate filters. GFP was excited at 470 nm and detected through a 515 nm emission filter. DAPI was excitation at 350 nm and detected at 420 nm through emission filter.

2.10. TUNEL assay

Apoptosis was measured by the terminal deoxyribonucleotide transferase (TdT)-mediated dUTP nick-end labeling (TUNEL) detecting in situ DNA fragmentation. TUNEL staining was performed using the In Situ Cell Death Detection Kit (Roche) as described previously [34].

2.11. Annexin V-propidium iodide double staining

Enumeration of apoptotic cells was done using FITC-conjugated Annexin V (BD Pharmingen, San Jose, CA) and propidium iodide (PI). Cells were washed twice in cold PBS and resuspended in Annexin V-binding buffer (BD Pharmingen) at a concentration of 3×10^6 per ml. This suspension (100 μl) was stained with 5 μl of Annexin V-FITC and 5 μl PI. The cells were gently vortexed and incubated for 15 min at room temperature in the dark. After addition of 400 μl of binding buffer to each tube, cells were analyzed by flow cytometry.

2.12. Statistical analysis

Three or more separate experiments were performed. Statistical analysis was done by one way ANOVA. A p value <0.05 was considered to have pronounced difference between experimental and control groups.

3. Results

3.1. The solubility of RAIDD is sensitive to pH

Previously, we successfully purified RAIDD-FL and realized that its solubility is extremely sensitive to salt concentration, which is also an important factor for the formation of PIDDosome. High salt levels dramatically reduced the RAIDD aggregation and precipitation. However, reducing RAIDD aggregation did not promote complex formation. Instead, a low salt condition facilitated PIDDosome formation (data not shown). The salt dependence of PIDDosome formation promoted us to evaluate the role of pH in the solubility of RAIDD-FL using turbidity and aggregation assays [35]. Without adding additional salt to the standard gel-filtration buffer containing 150 mM NaCl, RAIDD was insoluble at pH 4–6 and slightly soluble at pH 6–8. In addition, a sharp increase in solubility was detected at pH 9–11 (Fig. 1A and B). pH dependent solubility assay analyzed by turbidity and proportion of aggregated RAIDD-FL clearly showed that solubility of RAIDD depend on the pH (Fig. 1A and B). The soluble portion of RAIDD in the solution at different pH was also analyzed by SDS-PAGE (Fig. 1B). The PAGE experiment also indicates that soluble portion of RAIDD is

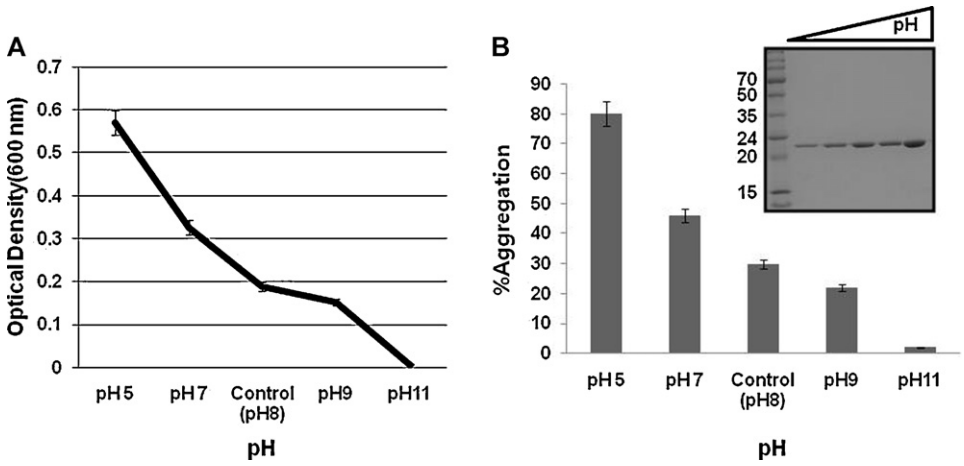

Fig. 1. The solubility of RAIDD is sensitive to pH. Solubility assay of pH effect on RAIDD-FL aggregation. (A) Turbidity of each sample incubated at different pH, as measured by the optical density at 600 nm. Values are means SD of $n = 3$. (B) Proportion of aggregated RAIDD-FL following incubation at various pH after centrifugation expressed as a percentage of the amount of the initial concentration of RAIDD. Protein concentration of the soluble portion of RAIDD in the solution was checked by a Bradford assay. Values are means SD of $n = 3$. The soluble portion of RAIDD in the solution was also loaded onto SDS-PAGE. Protein bands on a 15% SDS-PAGE gel were detected by Coomassie Blue staining. The migration of molecular size marker is indicated on the left side.

increased as pH increased. Because the isoelectric point of RAIDD is at pH 6.8, it is possible that the higher solubility at high pH is due to the shifting of the pH away from the isoelectric point.

3.2. RAIDD solubility based on pH directly influences the formation of PIDDosome

Because RAIDD solubility is extraordinarily sensitive to pH, we investigated the effect of pH on the PIDDosome formation and attempted to identify the optimal pH for complex formation. To accomplish this, separately purified RAIDD-FL and PIDD DD were mixed, incubated for 60 min at room temperature and then applied to a gel filtration column that had been pre-equilibrated with different pH buffers containing 50 mM NaCl and 1 mM DTT. The complex of RAIDD-FL and PIDD DD was then obtained by gel filtration chromatography. The profile of the gel filtration chromatography showed that PIDDosome formation was maximized at pH 8.0, whereas the complex was not produced at either pH 6.0 or 7.0 (Fig. 2). Although the complex was detected at pH 9.0, the amount was relatively small. Based on this result, we conducted all of the following peptides experiments in vitro at using buffer containing 20 mM Tris pH 8.0 and 50 mM NaCl.

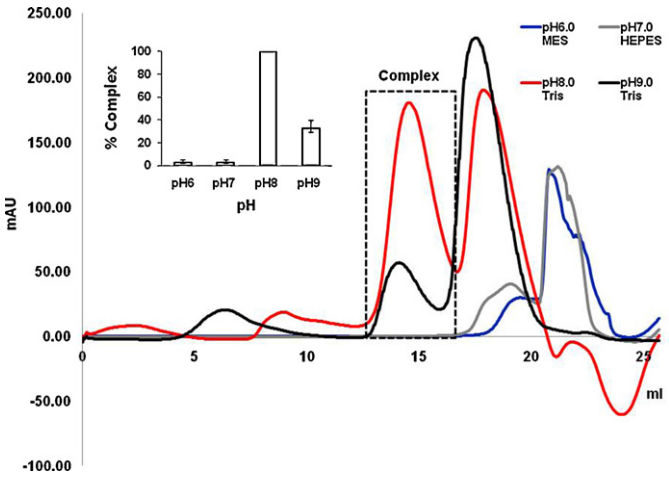

Fig. 2. PIDDosome formation is directly affected by the solubility of RAIDD. The profile from gel filtration chromatography shows that PIDDosome formation was maximized at pH 8.0 (shown in red), whereas the complex was not produced at either pH 6.0 or 7.0 (shown in blue and grey respectively). Approximately equal amounts of RAIDD-FL and PIDD DD were mixed and then incubated at room temperature for 60 min before being applied to a gel filtration column (shown in red) (absorption at 280 nm, indicated as milliabsorbance units (mAU)). Proportion of the complex formed at different pH is shown as bar-graph. Values are the means ± SD, $n = 3$. The amount of complex formed at pH 8.0 was considered to be 100% complex. Little complex also formed at pH 9. (For interpretation of the references to color in this figure legend, the reader is referred to the web version of the article.)

3.3. Rational design of TAT-fused peptides based on the structure of RAIDD DD and PIDD DD

We recently elucidated the crystal structure of the RAIDD DD:PIDD DD complex, which is in the core of the PIDDosome [20], and identified the dominant negative mutants as R147E on RAIDD DD and Y814A on PIDD DD [33]. Structure-based mutagenesis studies have shown that the presence of a point mutation on RAIDD DD (R147 to E147:R147E) and on PIDD DD (Y814 to A814:Y814A) resulted in their failing to form the PIDDosome complex [33]. Moreover, those mutants possess a dominant negative effect. The previous complex structure showed that R147 on RAIDD DD and Y814 on PIDD DD, located at the interface of the protein interaction, are critical for the PIDDosome assembly and conserved among RAIDD DDs and PIDD DDs across species (Fig. 3A). Based on previous structural and biochemical studies, we generated peptides that can still inhibit PIDDosome formations possessing a dominant negative effect and possibly inhibit genotoxic stress mediated apoptosis by disrupting PIDDosome assembly. In this method, target peptides are fused with the TAT sequence to give them the potential for cell penetration [36,37]. Cell-permeable peptides containing RAIDD helix3 (known as TAT-R147E) and PIDD helix3 (known as TAT-Y814A) fused to the internalization sequence of the TAT transactivator domain (YGRKKRRQRRR) at their N-terminus were synthesized and purified. Linker (GGG) was introduced in between the TAT sequence and the helix. The location of R147 on RAIDD DD and Y814 on PIDD DD in the interaction interface of the PIDDosome core complex and the sequence of TAT fused peptides generated based on the dominant negative mutants are shown in Fig. 3B and C.

3.4. TAT-Y814A and TAT-R147E inhibit PIDDosome formation in vitro

To analyze the effect of the synthesized peptides on the formation of PIDDosome in vitro, we conducted Native-PAGE and gel filtration chromatography. Purified RAIDD-FL and RAIDD DD

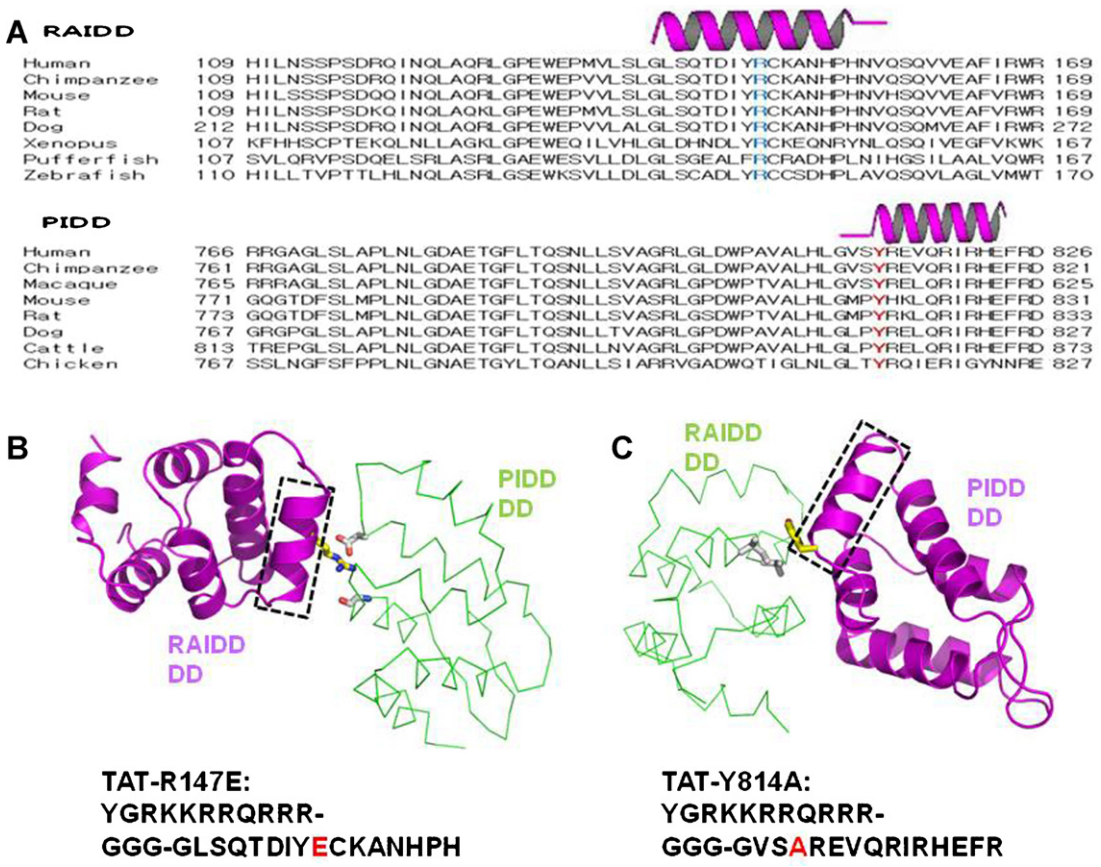

Fig. 3. Rational design of TAT-fused peptides based on RAIDD DD and PIDD DD. (A) Sequence alignment of RAIDD and PIDD from different species. The conserved residues, R147 on RAIDD and Y814 on PIDD, are shown as blue and red, respectively. The location of helix 3 (H3) is shown in the cartoon. B, The location of R147 on RAIDD DD and Y814 on PIDD DD in the interaction interface of the PIDDosome core complex are shown in the cartoon. The identities of each molecule are labeled. The sequence of TAT fused peptides generated based on the dominant negative mutants are indicated below the cartoon. (For interpretation of the references to color in this figure legend, the reader is referred to the web version of the article.)

were incubated with TAT-Y814A and PIDD DD was incubated with TAT-R147E followed by Native-PAGE. The absence of a complex band following Native-PAGE and the absence of a complex peak on the gel filtration profile clearly demonstrated that both novel TAT-fused peptides including mutants designed from RAIDD DD and PIDD DD failed to form a complex with their binding partner.

Next, we further evaluated those peptides to determine if they still possessed a dominant negative effect on formation of the PIDDosome. To accomplish this, approximately equal amounts of TAT-R147E or TAT-Y814A were mixed with wild-type RAIDD-FL or RAIDD DD and PIDD DD simultaneously and then incubated at room temperature for 60 min prior to being applied to the Native-PAGE. The complex formation and inhibition by peptides were then evaluated based on the appearance and disappearance of a new complex band. Incubation of purified RAIDD DD and PIDD DD with TAT-R147E did not cause a dramatic decrease in the complex band. However, incubation with TAT-Y814A caused almost complete disappearance of the band (Fig. 4A). The inhibitory effect of TAT-Y814A was stronger than that of TAT-R147A (Fig. 4A). In the case of using RAIDD-FL instead of RAIDD-DD, both peptides completely inhibited complex formation (Fig. 4B).

Since TAT-Y814A can lead to a dramatic effect on the complex formation between RAIDD-FL and PIDD DD, we further investigated the effect of the TAT-Y814A peptide dose. Specifically, we examined the decrease in the complex band in the presence of different concentrations of TAT-Y814A peptide by Native PAGE. To accomplish this, the complex was purified and mixed with different concentrations of TAT-Y814A and then incubated at room temperature for 60 min. The mixtures were then loaded onto a Native-PAGE. As shown in Fig. 4C and D, treating a mixture of 10 mg ml^{-1} RAIDD DD and PIDD DD with same amount of TAT-Y814A (1/1) inhibited the complex formation almost completely. These results clearly demonstrated that the inhibitory effects are dose dependent (Fig. 4C and D).

The inhibitory function of the TAT-Y814A peptide was further confirmed by gel-filtration chromatography (Fig. 4E). When we applied a mixture of RAIDD-FL and PIDD DD without peptide to the gel filtration column (S-200, GE Healthcare), the mixture formed the maximum amount of the complex. In contrast, the peptide mixture caused a decrease in the height of the complex peak. These findings indicated that both peptides, TAT-R147E and TAT-Y814A, generated based on RAIDD DD and PIDD DD, respectively, still possess a dominant negative mutant effect that interferes with the formation of a complex between RAIDD-FL or RAIDD DD and PIDD DD.

Finally, we analyzed peptide effect on the complete PIDDosome, which contains RAIDD-FL, PIDD DD, and caspase-2 CARD. Reconstitution of ternary complex was already introduced at previous study [37]. As increased the concentration of TAT-Y814A peptide on the ternary complex, the complex band obviously disappeared and dissociated RAIDD and PIDD DD bands were appeared on the Native-PAGE (Fig. 4F).

3.5. Transduction of recombinant TAT-fused peptides into Caki cells

Using FITC-labeled peptides, we tested the capability and efficacy of the TAT fused peptides to cross the membranes of Caki

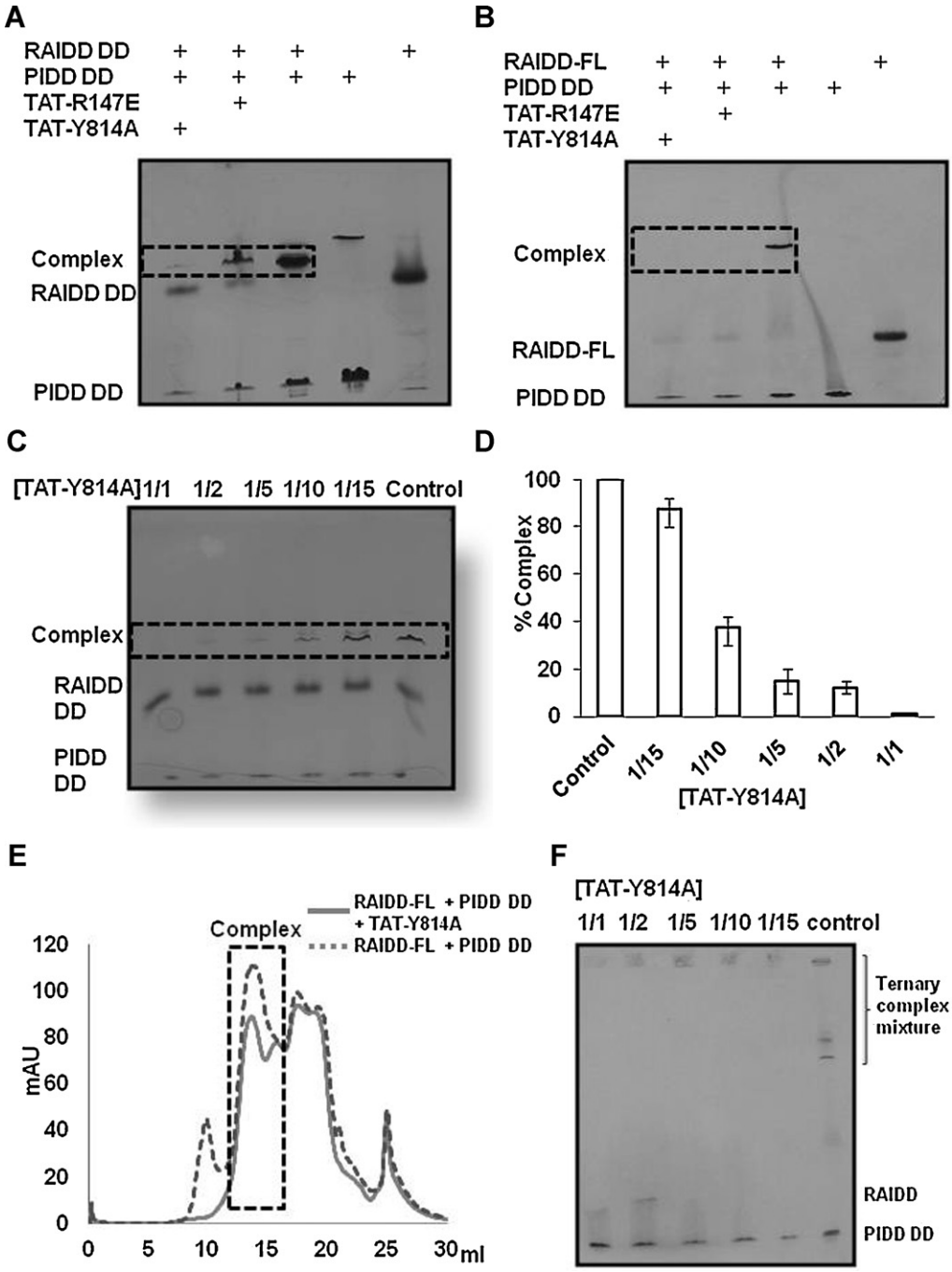

Fig. 4. TAT-Y814A and TAT-R147E inhibit PIDDosome formation in vitro. (A) Purified RAIDD DD, PIDD DD, RAIDD DD + PIDD DD mixture, and RAIDD DD + PIDD DD mixture + TAT fused peptide mixture were pre-incubated for 60 min at room temperature, after which the mixtures were subjected to Native-PAGE. The complex formation and inhibition by peptides were then evaluated based on the appearance and disappearance of a new complex band. Newly appeared complex bands made of RAIDD-FL and PIDD DD as well as RAIDD-FL and PIDD DD alone are indicated. (B) The Native-PAGE experiment was conducted using the same method as used for A; however, RAIDD-FL was used instead of RAIDD DD. (C) TAT-Y814A dose dependent inhibition of PIDDosome formation. RAIDD DD:PIDD DD complex was prepared and mixed with various different concentrations of TAT-Y814A peptide as indicated above the gel, after which the mixtures were subjected to Native-PAGE. (D) % of the complex was evaluated based on the appearance and thickness of the band generated by the complex. Thickness of the complex band formed in the control without any peptide was considered to be 100% complex. (E) The profile from gel filtration chromatography showed an inhibitory effect of TAT-Y814A on the formation of PIDDosome. Approximately equal amounts of TAT-Y814A were mixed with an equal amount of wild-type PIDD DD and RAIDD-FL simultaneously and then incubated at room temperature for 60 min before injection. The mixture of wild type RAIDD DD and PIDD DD without any mutants was used as a control (shown as dashed line). All complex positions in this figure are boxed with a dashed line. (F) TAT-Y814A dose dependent inhibition of ternary PIDDosome formation. Ternary PIDDosome complex, which includes RAIDD-FL, PIDD DD, and caspase-2 CARD, was prepared and mixed with various different concentrations of TAT-Y814A peptide as indicated above the gel, after which the mixtures were subjected to Native-PAGE.

cells. The cells were inspected via fluorescence microscopy for the specific intracellular accumulation of a fluorescent signal after 24 h of incubation. As shown in Fig. 5, the TAT-R147E, TAT-Y814A or TAT-DREP2 efficiently transduced Caki cell lines to a level of almost 100% after 24 h of incubation. These results demonstrate the efficient transduction of TAT-fused peptides into Caki cells.

3.6. TAT-Y814A and TAT-R147E partially inhibit apoptosis induced by cisplatin treatment in Caki cells

We demonstrated the ability of transduced recombinant TAT-R147E and TAT-Y814A to inhibit the intrinsic apoptotic pathway induced by 32 μg/ml cisplatin and assessed the level of apoptotic

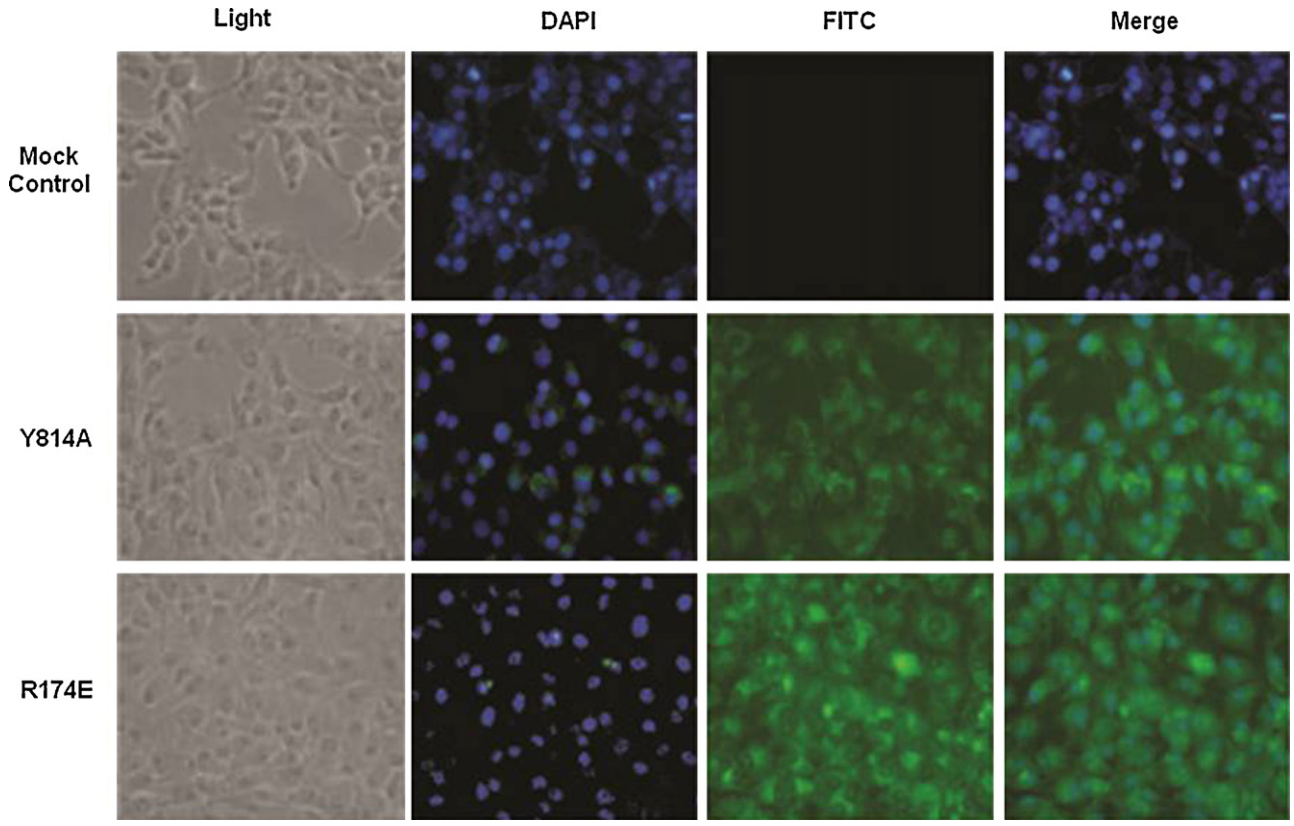

Fig. 5. Transduction of TAT-fusion peptides into Caki cells. The recombinant TAT-fusion peptides, TAT-Y814A and TAT-R147E, and TAT-DREP2 were labeled with FITC and incubated with cultured cells for 24 h. After Caki cells were incubated with the TAT-fused peptides for 24 h, the cells were fixed with 1% paraformaldehyde for 30 min at room temperature. After washing with PBS, 300 nM DAPI (4′,6′-diamidino-2-phenylindole, Roche, Germany) was added to the fixed cells for 5 min. The uptake and intracellular distribution were monitored by fluorescence microscopy with the appropriate filters.

cells by flow cytometry in Caki cells. 60 min after pre-incubation with 50 μM TAT-R147E, TAT-Y814A and TAT-DREP2, cells were stimulated concomitantly with cisplatin for 24 h. DREP2 (the regulator of apoptotic DNA fragmentation in fly) derived TAT-fused peptide (YGRKKRRQRRRGGGEYFRTLANNTVLLLLR) was used for control experiment. As shown in Fig. 6A, TAT-R147E and TAT-Y814A slightly reduced the cleavage of procaspase-2 and procaspase-3 in Caki cells in response to cisplatin treatment, but not DREP2. Cleaved form of caspase-3 was also reduced after treatment of our peptides (Fig. 6A). Treatment of Caki cells with cisplatin resulted in a markedly increased accumulation of sub-G1 phase cells when compared to control cells. Pretreatment with TAT-R147E and TAT-Y814A partially blocked cisplatin-induced apoptosis (Fig. 6B and C). As shown in Fig. 6C, the inhibitory effects of TAT-Y814A on genotoxic stress-induced apoptosis were relatively stronger than those of TAT-R147E. Taken together, these results suggested that the inhibitory effect of TAT-R147E and TAT-Y814A on cisplatin-mediated caspase-2 activation attenuated cisplatin induced-apoptosis.

To analysis our peptides effect more quantitative way, we conducted a TAT-peptide concentration-dependent assay. As shown in Fig. 7A, pretreatment with TAT-Y814A blocked cisplatin-induced apoptosis both at low dosage of cisplatin (24 μg/ml) and at high dosage of cisplatin (32 μg/ml). The inhibitory effects of TAT-Y814A on genotoxic stress-induced apoptosis were almost same above 50 μM of TAT-Y814A. We also performed TUNEL assay to quantify the apoptotic cells and obtained similar result with that from FACS (Fig. 7B). Next, we examined the translocation of membrane phosphatidylserine from the inner to outer leaflet of the plasma membrane to quantify the apoptotic cells. As shown in Fig. 7C, the incidence of late apoptotic PI^+/Annexin V^+ cells were increased in cisplatin-treated cells although the incidence of necrotic PI^+/Annexin V^- cells was increase by cisplatin treatment. In addition, pretreatment with Y814A or R174E PTD-peptides decreased the population of late apoptotic PI^+/Annexin V^+ cells as well as PI^+/Annexin V^- necrotic cells increased by cisplatin treatment. These results confirmed that cisplatine-induced cell death was blocked by TAT-R147E and TAT-Y814A PDT-peptides.

4. Discussion

Since the caspase-2 activating complex, PIDDosome, mediated genotoxic induced apoptosis, specific inhibitors of this protein complex should have therapeutic potential. To develop chemicals and peptide inhibitors that specifically suppress genotoxic stress mediated apoptosis, we have been biochemically and structurally investigating PIDDosome [38,39]. During previous studies, we realized that the complex formation between RAIDD DD and PIDD DD is sensitive to the buffer and environmental conditions such as salt concentration, incubation time, and temperature [39]. Previously, we also found that the solubility of successfully purified full length RAIDD (named RAIDD-FL) is extremely sensitive to salt concentration, which is an important factor involved in the formation of PIDDosome [39]. The salt dependence of PIDDosome formation and the solubility of RAIDD-FL promoted us to evaluate the role of pH in the solubility of RAIDD-FL and formation of PIDDosome composed of RAIDD-FL and PIDD DD to determine the optimal conditions for complex formation. This step was necessary for the following studies with peptides. RAIDD with 150 mM NaCl was insoluble at pH 4–6 and slightly soluble at pH 6–8. A sharp increase in solubility occurred at pH 9–11. Because the isoelectric point of RAIDD is at pH 6.8, it is possible that the higher

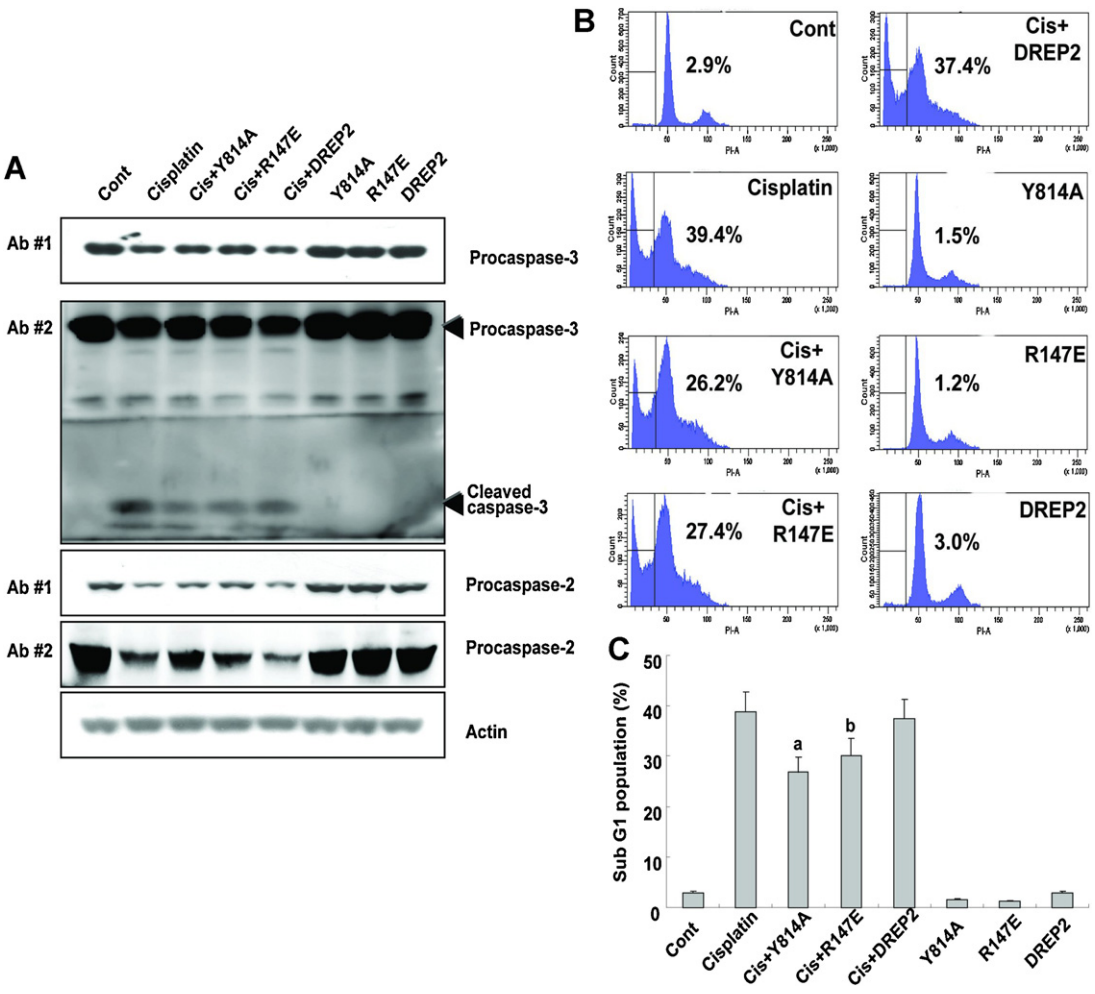

Fig. 6. TAT-Y814A and TAT-R147E partially inhibit apoptosis induced by cisplatin treatment in Caki cells. (A) TAT-Y814A and TAT-R147E partially suppress the cleavage of procaspase-2 and -3 induced by cisplatin treatment in Caki cells. After TAT fused peptides were pre-incubated for 60 min, the cells were treated with cisplatin for 24 h. Equal amounts of cell lysates (40 μg) were subjected to electrophoresis and analyzed by Western blot for procaspase-2, procaspase-3, and actin for normalization. We used two different antibodies for caspase-2 and caspase-3 to detect pro-form and the cleaved forms. (B) TAT-Y814A and TAT-R147E partially inhibit apoptosis induced by cisplatin treatment in Caki cells. After TAT fused peptides were pre-incubated for 60 min, the cells were treated with cisplatin. After 24 h, apoptosis was analyzed as a sub-G1 fraction by FACS. A representative study is shown; two additional experiments yielded similar results. (C) Graph of sub-G1 population. Data shown are means ± SD ($n = 3$). [a]$p < 0.05$ for cisplatin-treated cells *versus* Cis + Y184A-, or Cis + R174E-treated cells by ANOVA.

solubility at low pH is due to the shifting of the pH away from the isoelectric point. Based on the characteristics of RAIDD-FL obtained during our preliminary experiment, we investigated the effect of pH on PIDDosome formation. The results of our study revealed that PIDDosome formation was maximized at pH 8.0. Conversely, only a small amount of complex was formed at pH 9, and the complex was not produced at either pH 6.0 or 7.0, which indicates that complex formation between RAIDD-FL and PIDD DD is significantly influenced by pH and the optimal pH for formation of the complex is around 8.0. Based on this biochemical assay, we investigated the following peptide experiments conducted in vitro in buffer containing 20 mM Tris pH 8.0 and 50 mM NaCl.

We recently elucidated the crystal structure of the RAIDD DD:PIDD DD complex and identified dominant negative mutants. Structure-based mutagenesis studies have shown that DDs containing a point mutation on RAIDD DD (R147 to E147:R147E) and on PIDD DD (Y814 to A814:Y814A) negatively inhibited PIDDosome formation. Based on previous structural and biochemical studies, we attempted to generate peptides that could still inhibit PIDDosome formations exerting a negative effect and possibly inhibit genotoxic stress mediated apoptosis by disrupting the PIDDosome assembly. In the current study, we identified mutant peptides derived from R147A (RAIDD mutant) and Y814A (PIDD mutant) that contain helix 3 of both DDs (amino acids 139–156 of RAIDD and 811–825 of PIDD), suppress PIDDosome formation in vitro and suppress genotoxic stress induced apoptosis in vivo. A membrane-penetrating peptide, TAT (YGRKKRRQRRR), was used for in vivo experiments. Cell-permeable peptides containing RAIDD helix3 (named TAT-R147E) and PIDD helix3 (named TAT-Y814A) fused to the internalization sequence of the TAT transactivator domain at their N-termini clearly negatively inhibited PIDDosome formation in vitro. The inhibitory effects of TAT-Y814A on PIDDosome formation and genotoxic stress-induced apoptosis were stronger than those of TAT-R147E.

The novel TAT-fused peptides, TAT-R147E and TAT-Y814A, which had a negative effect on PIDDosome formation, might be good candidates for peptide drugs that can inhibit genotoxic stress induced apoptosis by interfering with the assembly of PIDDosome. p53 tumor suppressor is a key mediator of stress response that protects normal cells from altering potentially dangerous cancer cells by inducing apoptosis in especially genotoxically damaged cells. Although p53 performs a critical role in cells, under certain conditions, p53 activity can result in massive apoptosis, leading to severe pathological consequences. For example, anti-cancer

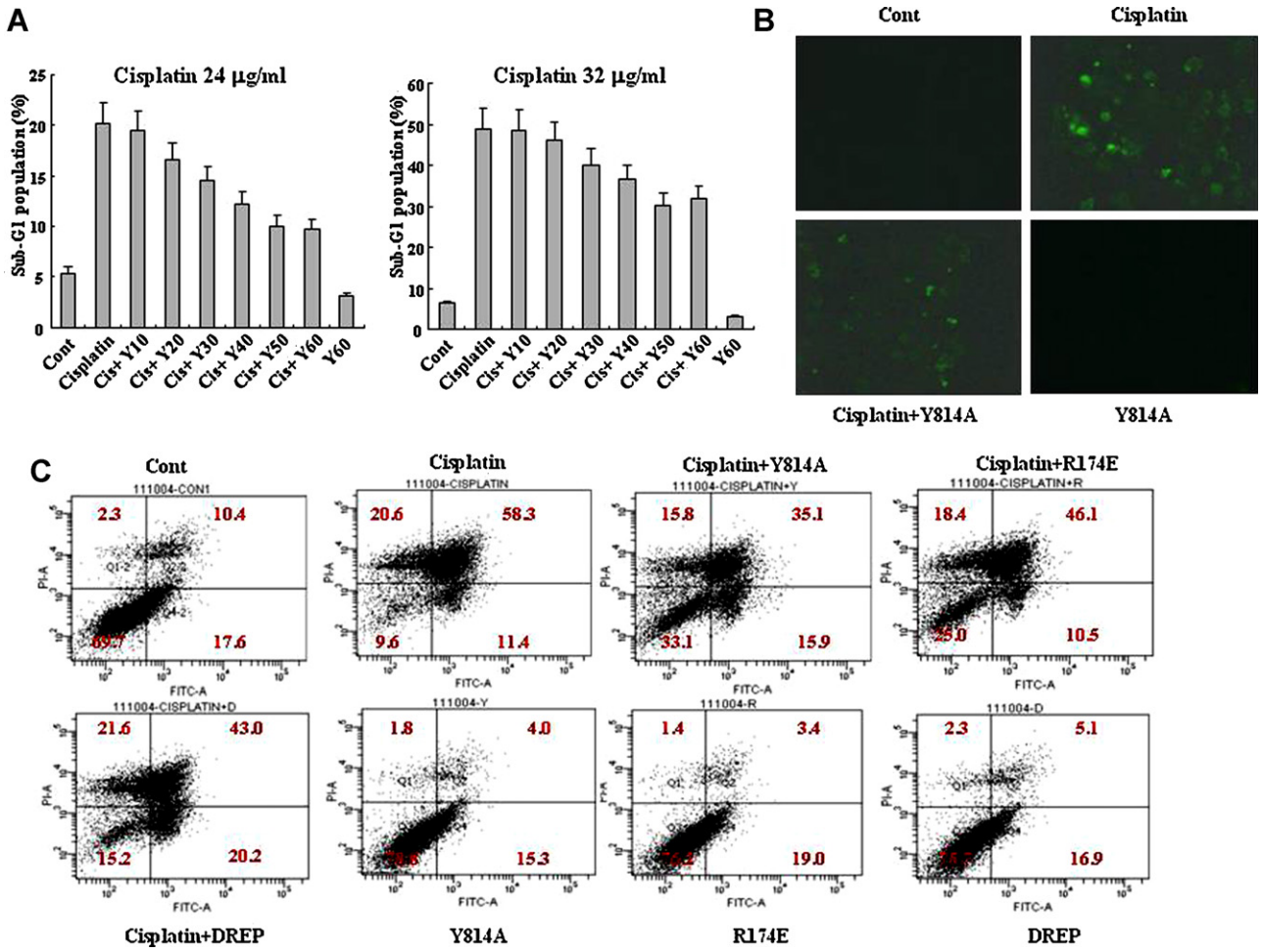

Fig. 7. TUNEL assay and Annexin V-propidium iodide double staining assay to quantify the apoptotic cells. (A) TAT-fused peptide concentration-dependent effect for cisplatin induced apoptosis. After TAT-fused peptides were pre-incubated for 60 min, the cells were treated with cisplatin (24 μg/ml or 32 μg/ml). After 24 h, apoptosis was analyzed as a sub-G1 fraction by FACS. A representative study is shown; two additional experiments yielded similar results. Y10 ~ Y60 indicate the concentration of peptides, ex. Y10 = 10 μm Y814A. (B) TUNEL assay. The Caki cells were cultured in cover glass for 36 h. After TAT-fused peptides were pre-incubated for 60 min, the cells were treated with cisplatin for 24 h. Cells were fixed with 4% paraformaldehyde and subsequently permeabilized with PBS containing 0.1% Triton X. After incubation with the TUNEL reaction mixture, cells were examined using fluorescence microscopy. Production of green fluorescent indicates TUNEL positive cells. (C) Annexin V-propidium iodide double staining assay. Caki cells were treated with cisplatine alone or cisplatine Y814A or R174E PTF-peptides for 24 h, harvested, and stained with PI and Annexin V. Cell death was determined by flow cytometry. Bottom right quadrant, Annexin V^+, early apoptotic cells; top right quadrant, Annexin V^+/PI^+, late apoptotic cells. Values correspond to the percentage of cells in those quadrants. Two additional studies yielded equivalent results.

therapy is often associated with genotoxic stress, leading to excessive apoptosis. Numerous reports have suggested that inhibition or activation of apoptosis by small molecules and peptides might be therapeutic [40–43]. We showed that TAT-R147E and TAT-Y814A inhibited PIDDosome formation and could desensitize the cells to apoptosis induced by cisplatin. Thus, the peptides derived from RAIDD and PIDD reported here have wide ranging therapeutic potential.

Conversely, elimination of complex constituents PIDD or RAIDD did not significantly influence caspase-2 activation [24]. These previous reports suggested alternative mechanisms to the PIDDosome for caspase-2 activation in response to DNA damage [24]. In the present study, despite TAT-R147E and TAT-Y814A inhibiting PIDDosome formation and cisplatin-induced caspase activation, the in vivo effects were not as strong as the in vitro effects. Thus, further studies are needed to clarify the underlying mechanism(s) of PIDDosome-independent caspase-2 processing in response to genotoxic stress.

In conclusion, our findings suggest that dominant negative mutant of PIDD and RAIDD inhibit PIDDosome formation in vitro and attenuates genotoxic stress-induced apoptosis in human renal cancer cells. These results suggest that TAT-Y814A or TAT-R147E is a novel inhibitor of genotoxic stress-induced apoptosis and may serve as a prototype for anti-apoptotic drug development.

Acknowledgement

This study was supported by a grant from the Korea Healthcare Technology R&D Project, Ministry of Health & Welfare, Republic of Korea (A100190).

References

[1] Jacobson MD, Weil M, Raff MC. Programmed cell death in animal development. Cell 1997;88:347–54.
[2] Park HH, Lo YC, Lin SC, Wang L, Yang JK, Wu H. The death domain superfamily in intracellular signaling of apoptosis and inflammation. Annu Rev Immunol 2007;25:561–86.
[3] Thompson CB. Apoptosis in the pathogenesis and treatment of disease. Science 1995;267:1456–62.
[4] Oliveira JB, Gupta S. Disorders of apoptosis: mechanisms for autoimmunity in primary immunodeficiency diseases. J Clin Immunol 2008;28(Suppl. 1):S20–8.
[5] Iwahashi H, Eguchi Y, Yasuhara N, Hanafusa T, Matsuzawa Y, Tsujimoto Y. Synergistic anti-apoptotic activity between Bcl-2 and SMN implicated in spinal muscular atrophy. Nature 1997;390:413–7.
[6] Denault JB, Salvesen GS. Caspases: keys in the ignition of cell death. Chem Rev 2002;102:4489–500.

[7] Nicholson DW. Caspase structure, proteolytic substrates, and function during apoptotic cell death. Cell Death Differ 1999;6:1028–42.
[8] Salvesen GS, Dixit VM. Caspases: intracellular signaling by proteolysis. Cell 1997;91:443–6.
[9] Salvesen GS. Caspases and apoptosis. Essays Biochem 2002;38:9–19.
[10] Chao Y, Shiozaki EN, Srinivasula SM, Rigotti DJ, Fairman R, Shi Y. Engineering a dimeric caspase-9: a re-evaluation of the induced proximity model for caspase activation. PLoS Biol 2005;3:1079.
[11] Salvesen GS, Dixit VM. Caspase activation: the induced-proximity model. Proc Natl Acad Sci USA 1999;96:10964–7.
[12] Shi Y. Caspase activation: revisiting the induced proximity model. Cell 2004;117:855–8.
[13] Donepudi M, Mac Sweeney A, Briand C, Grutter MG. Insights into the regulatory mechanism for caspase-8 activation. Mol Cell 2003;11:543–9.
[14] Carrington PE, Sandu C, Wei Y, Hill JM, Morisawa G, Huang T, et al. The structure of FADD and its mode of interaction with procaspase-8. Mol Cell 2006;22:599–610.
[15] Adams JM, Cory S. Apoptosomes: engines for caspase activation. Curr Opin Cell Biol 2002;14:715–20.
[16] Acehan D, Jiang X, Morgan DG, Heuser JE, Wang X, Akey CW. Three-dimensional structure of the apoptosome: implications for assembly, procaspase-9 binding, and activation. Mol Cell 2002;9:423–32.
[17] Franchi L, Eigenbrod T, Munoz-Planillo R, Nunez G. The inflammasome: a caspase-1-activation platform that regulates immune responses and disease pathogenesis. Nat Immunol 2009;10:241–7.
[18] Martinon F, Burns K, Tschopp J. The inflammasome: a molecular platform triggering activation of inflammatory caspases and processing of proIL-beta. Mol Cell 2002;10:417–26.
[19] Tinel A, Tschopp J. The PIDDosome, a protein complex implicated in activation of caspase-2 in response to genotoxic stress. Science 2004;304:843–6.
[20] Park HH, Logette E, Rauser S, Cuenin S, Walz T, Tschopp J, et al. Death domain assembly mechanism revealed by crystal structure of the oligomeric PIDDosome core complex. Cell 2007;128:533–46.
[21] Baliga BC, Read SH, Kumar S. The biochemical mechanism of caspase-2 activation. Cell Death Differ 2004;11:1234–41.
[22] Kim IR, Murakami K, Chen NJ, Saibil SD, Matysiak-Zablocki E, Elford AR, et al. DNA damage- and stress-induced apoptosis occurs independently of PIDD. Apoptosis 2009;14:1039.
[23] Manzl C, Krumschnabel G, Bock F, Sohm B, Labi V, Baumgartner F, et al. Caspase-2 activation in the absence of PIDDosome formation. J Cell Biol 2009;185:291–303.
[24] Olsson M, Vakifahmetoglu H, Abruzzo PM, Hogstrand K, Grandien A, Zhivotovsky B. DISC-mediated activation of caspase-2 in DNA damage-induced apoptosis. Oncogene 2009;28:1949–59.
[25] Lin Y, Ma W, Benchimol S. Pidd, a new death-domain-containing protein, is induced by p53 and promotes apoptosis. Nat Genet 2000;26:122–7.
[26] Bergeron L, Perez GI, Macdonald G, Shi L, Sun L, Jurisicova A, et al. Defects in regulation of apoptosis in caspase-2-deficient mice. Genes Dev 1998;12:1304–14.
[27] Lassus P, Opitz-Araya X, Lazebnik Y. Requirement for caspase-2 in stress-induced apoptosis before mitochondrial permeabilization. Science 2002;297:1352–4.
[28] Robertson JD, Enoksson M, Suomela M, Zhivotovsky B, Orrenius S. Caspase-2 acts upstream of mitochondria to promote cytochrome c release during etoposide-induced apoptosis. J Biol Chem 2002;277:29803–9.
[29] Tinel A, Janssens S, Lippens S, Cuenin S, Logette E, Jaccard B, et al. Autoproteolysis of PIDD marks the bifurcation between pro-death caspase-2 and pro-survival NF-kappaB pathway. EMBO J 2006;26:197–208.
[30] Janssens S, Tinel A, Lippens S, Tschopp J. PIDD mediates NF-kappaB activation in response to DNA damage. Cell 2005;123:1079–92.
[31] Duan H, Dixit VM. RAIDD is a new 'death' adaptor molecule. Nature 1997;385:86–9.
[32] Weber CH, Vincenz C. The death domain superfamily: a tale of two interfaces? Trends Biochem Sci 2001;26:475–81.
[33] Jang TH, Bae JY, Park OK, Kim JH, Cho KH, Jeon JH, et al. Identification and analysis of dominant negative mutants of RAIDD and PIDD. Biochim Biophys Acta 2010;1804:1557–63.
[34] Bondos SE, Bicknell A. Detection and prevention of protein aggregation before, during, and after purification. Anal Biochem 2003;316:223–31.
[35] Ding B, Price RL, Goldsmith EC, Borg TK, Yan X, Douglas PS, et al. Left ventricular hypertrophy in ascending aortic stenosis mice: anoikis and the progression to early failure. Circulation 2000;101(24):2854–62.
[36] Silhol M, Tyagi M, Giacca M, Lebleu B, Vives E. Different mechanisms for cellular internalization of the HIV-1 Tat-derived cell penetrating peptide and recombinant proteins fused to Tat. Eur J Biochem 2002;269:494–501.
[37] Vives E, Brodin P, Lebleu B. A truncated HIV-1 Tat protein basic domain rapidly translocates through the plasma membrane and accumulates in the cell nucleus. J Biol Chem 1997;272:16010–7.
[38] Park HH. Structural analyses of death domains and their interactions. Apoptosis 2011;16:209–20.
[39] Jang TH, Zheng C, Wu H, Jeon JH, Park HH. In vitro reconstitution of the interactions in the PIDDosome. Apoptosis 2010;15:1444–52.
[40] Choi M, Rolle S, Wellner M, Cardoso MC, Scheidereit C, Luft FC, et al. Inhibition of NF-kappaB by a TAT-NEMO-binding domain peptide accelerates constitutive apoptosis and abrogates LPS-delayed neutrophil apoptosis. Blood 2003;102:2259–67.
[41] Fischer U, Schulze-Osthoff K. Apoptosis-based therapies and drug targets. Cell Death Differ 2005;12(Suppl. 1):942–61.
[42] Wang S. The promise of cancer therapeutics targeting the TNF-related apoptosis-inducing ligand and TRAIL receptor pathway. Oncogene 2008;27:6207–15.
[43] Letai A, Bassik MC, Walensky LD, Sorcinelli MD, Weiler S, Korsmeyer SJ. Distinct BH3 domains either sensitize or activate mitochondrial apoptosis, serving as prototype cancer therapeutics. Cancer Cell 2002;2:183–92.